COMPARISON OF HONEYCOMB PLATE MODELS USING MSC/NASTRAN*

Paul F. Martin
Massachusetts Institute of Technology
Lincoln Laboratory
Lexington, Massachusetts 02173-9108

ABSTRACT

An evaluation of a two-inch-thick, one-way honeycomb optical bench is performed with MSC/NASTRAN. Geometry of the bench is such that its behavior may be predicted by flat-plate analysis. Aspect ratios of the bench are set such that shear deformation is not negligible. The core of the bench is a honeycomb with a 2-inch-square mesh. This core is connected to top and bottom cover plates. The evaluation of the bench is performed with five different models. In the first, the cover plates and all ribs are represented with CQUAD elements. The second and third use a single layer of CQUAD elements whose properties are given with PSHELL and PCOMP. The fourth uses a single layer of CQUAD elements combined with CBEAMS for the ribs. The fifth uses a single set of CBEAMS which lie along the longitudinal axis. Static and dynamic responses are obtained.

I. INTRODUCTION

Analysis of a bench which behaves as a flat one-way plate with finite elements using MSC/NASTRAN is normally performed with the use of the CQUAD element. When the flat plate is built with a honeycomb core, the analysis can be more rigorous. The honeycomb core can be represented as an interlaminar shear layer (using PCOMP) or the entire core can be discretized and modeled. The option also exists to model the bench with a single layer of CQUAD elements and modify the inertia and shear properties to account for the core. A variation on this method is to model the cover plates with a single layer of CQUAD elements and the ribs with CBEAMS elements. For behavior as a one-way span, evaluation as a beam is also possible with appropriate section properties. Since the mathematical models are not identical, the results may vary.

Discretization of the honeycomb core into individual separate finite elements would most closely represent the actual system. However, because of the number of degrees of freedom involved in this model (as opposed to the single layer of CQUADS or CBEAMS), the execution time would be long. The results of such an analysis are presented and comparisons are made of the results of the four other methods of representing the honeycomb bench.

---

*This work was sponsored by the Department of the Air Force.

II. BACKGROUND

This evaluation stems from analysis of the LITE* Optical Module (OM) which consists of a set of optical components mounted on an optical bench. A mathematical model of the OM has been developed. At present there are two mathematical models of the LITE OM. The differences between the two models lie in the representation of the optical bench. In one, the All-Up Model, the bench is represented as a discretized 3D honeycomb model in which all honeycomb ribs and cover plates are represented with CQUAD elements. The complexity of the All-Up Model results in an enormous execution time. A task for reducing this model to superelements has been undertaken to facilitate its execution. A simpler representation of the bench in the model of the LITE OM is the Bar-Bench Model. In this model the bench representation consists of a longitudinal bar (comprised of CBAR elements) oriented along the major axis of the bench with appropriate section properties of the bench. The Bar-Bench is more concise and requires significantly less execution time. Representation of the bench as a single layer of plate elements with appropriate section properties would require substantially less execution time than the All-Up Model. In fact the execution time could possibly be reduced to approximately 1/4 of that required for the larger model by cutting the number of nodes in half. This task of reducing the bench to a single layer of plate elements could be done if the representation provided satisfactory results.

Both models of the bench were evaluated for frequency content as stand-alone models (i.e., bench only with all other portions of system removed). A comparison between modal frequencies of the two stand-alone bench models is shown as Table 1.

TABLE 1
LITE STAND-ALONE OPTICAL BENCH RESONANCES (Hz)

Mode	All-Up Model	Bar-Bench Model
1	1306.3	1640.6
2	1467.7	2044.3
3	3270.0	2098.3

The LITE optical bench is shown as Fig. 1. The LITE optical bench has an aspect ratio (length to thickness) which might lend itself to analysis as a one-way span. However, the cross-section aspect ratios (length to width) of this one-way span would seem to indicate that a plate analysis might be more prudent. This analysis investigated the validity of using various models to represent a honeycomb plate.

The LITE optical bench serves as a mounting platform for various small optical components. Therefore, the effect of the models on small bench-mounted oscilator response was also investigated.

*Laser Intersatellite Transmission Experiment

III. GENERAL DESCRIPTION OF MODELS

The system to be represented is an 8 x 16 x 2 in. honeycomb bench. The specifications for the bench are as below. The material for the structure is aluminum ($E = 10. \times 10^6$ psi, $RHO = 2.54 \times 10^{-4}$ #-sec^2/in^4). The honeycomb core consists of longitudinal ribs 2 in. deep, 0.06 in. thick, spaced at 2 in. on center. The ribs extend for the full length and width of the bench.

top plate	0.06 in. thick
bottom plate	0.06 in. thick
ribs	0.06 in. thick spaced at 2 in. C/C.

The geometric details of the bench are based in general on the optical bench to be used in the LITE program.

The bench is modeled in the five different methods described below.

Three-Dimensional Honeycomb Model (3D)

For this evaluation the honeycomb bench was represented with three-dimensional model with CQUAD elements representing the top and bottom cover plates and elements representing the vertical ribs. The model is shown in Fig. 2. The results from the analysis of this model became the basis for evaluation with the other models.

The properties for the CQUAD elements are listed below:

PSHELL INPUT

Top cover plate	0.06 in.
Bottom cover plate	0.06 in.
Vertical honeycomb ribs	0.06 in.
Honeycomb rib spacing	2 in. c/c
Depth of section	2 in.

The resulting section properties of the total honeycomb bench (per inch) are listed below:

Area (per inch)	0.195 in^2
Strong Axis Inertia	9.752 in^4
Weak Axis Inertia (per inch)	0.145 in^4
Torsional Constant	3.072 in^4

Two-Dimensional Flat-Plate Model (2D)

The honeycomb bench has been represented by a flat-plate model. This model represents the bench as a single layer of CQUAD elements with appropriate section properties. This model is shown as Fig.3. The appropriate properties are specified on

a NASTRAN PSHELL card. The use of analyses with PSHELL properties is primarily intended for shell analysis(thus the name).[1] The section properties (bending and shear) are based on the membrane thickness of a solid section. There is a provision for including constants, R_1 for bending and R_t for shear, for modification of these properties when a composite or nonsolid section is being modeled. The constant for modification of the bending term is developed below.

PSHELL INPUT

Membrane thickness (t)	0.195 in
Inertia (I_o) based on t (per inch)	0.000828 in^4
Actual inertia (I) (per inch)	0.145 in^4
R_1 ($12I/t^3$)	234.66

Shear coefficient, R_t. is taken from Cowper [2], for square box sections, to be 0.437.

1D Beam Model (1D)

The honeycomb bench was represented by a single beam at the longitudinal axis of the bench. The model represents the bench as a single line of CBEAM elements with appropriate section properties. This model is shown as Fig. 4. The appropriate properties are those developed for the total honeycomb bench and are specified on a NASTRAN PBAR card.

PBEAM INPUT

Area	8 x 0.195	=	1.56 in^2
Iz		=	9.75 in^4
Iy	8 x 0.145	=	1.16 in^4
J		=	3.07 in^4

shear coefficient, from Cowper [2],

weak axis	$K_w = 0.437$
strong axis	$K_s = 0.833$

Composite Plate Model (C)

The honeycomb bench was represented as a flat layered composite plate. The model represents the bench as a single layer of CQUAD elements with appropriate section properties. The section properties are represented as a layered composite with appropriate properties specified on a NASTRAN PCOMP card. The PCOMP represents the core as a solid layer capable of transferring shear. Since it is actually representing a honeycomb core, an equivalent value of Young's modulus and mass density are developed based on cross-sectional area. These values are then used for input to a NASTRAN MAT1 card.

Cross-sectional area of honeycomb (A_h)
5 x 0.06 x 1.94 = 0.58 sq. in.

Cross-sectional area of solid core (A_e)
8. x 1.94 = 15.52 sq. in.

Modular Ratio $n = A_h/A_e = 0.58/15.58 = 0.04$

Honeycomb Properties (units: lb, inch, sec)

Youngs' Modulus	$E = 10.0 \times 10^6$ psi
Mass Density (rho)	$\rho = 2.53 \times 10^{-4}$

Equivalent Solid Core Properties

Young's Modulus	$nE = 4.00 \times 10^5$
Mass Density	$n\rho = 1.01 \times 10^{-5}$

This model is illustrated in Fig. 3 (the same as the 2D model).

In models 1D, 2D and C, transverse ribs are represented with concentrated masses.

Beam and Quad Model (BQ)

This model was generated based on the 2D model. The difference between the two lies in the representation of all of the ribs as beam elements. A single layer of CQUAD elements was used to represent both the top and bottom cover plates. Input for the PSHELL is listed below. The model is also shown as Fig. 5.

PSHELL INPUT

Membrane thickness (t)	0.120 in.
Inertia (I_o) based on t (per inch)	0.000144 in^4
Actual inertia (I) (per inch)	0.120 in^4
R_1 ($12I/t^3$)	833.33

shear coefficient, from Cowper [2], $R_t = 0.437$

The honeycomb ribs are represented by CBEAM elements. The properties used in the PBEAM cards are listed below:

PBEAM INPUT

Area	2.00 x .06	=	0.1200 in^2
Iy	$(2.00^3 \times .06)/12$	=	0.0400 in^4
Iz	$(0.06^3 \times 2.00)/12$	=	3.60×10^{-5} in^4
J	$(0.06^3 \times 2.00)/3$	=	1.44×10^{-4} in^4

Shear coefficients for the ribs in the strong axis are taken to be the same as those previously calculated.

Shear coefficients are:

exterior ribs $R_t = 0.833$
interior ribs $R_t = 0.437$

IV. ANALYSES

Several analyses were performed on the various representations of the bench, and they are listed below.

As noted, the bench supports a number of small optical components. In order to identify the effect of the various models on small oscillators, two single-degree-of-freedom oscillators (sdof) were attached to the various models. The oscillators were modeled to have stiffness and mass such that their resonances were at 600 Hz and 840 Hz. The 600-Hz oscillator has a mass of 0.0009 #-sec^2/in and is located along one midside free edge of the bench. The 840-Hz oscillator has a mass of 0.00045 #-sec^2/in and is located along the opposite free edge of the bench from the 600-Hz oscillator and 6 in. from one end. The oscillator resonant frequencies are representative of typical LITE optical components.

Both oscillators were rigidly attached to the bench. Attachment of the oscillators to the 3D model was accomplished with the use of multi-point constraints.

In the analyses the models were provided with boundary conditions to result in pinned ended one-way spans. This was done by supporting against translation all nodes along the neutral axis at either end of the plates.

Displacement Analysis

To evaluate the static response of the five models, a simple analysis was performed. A 1000-lb line loading was applied across the center of the span. The resulting displacements are described below.

TABLE 2
DISPLACEMENT UNDER 1000 LB LOAD

Model	Displacement At Midspan (in.)
1D	0.008900
2D	0.008685
3D	0.008720
C	0.008788
BQ	0.008685

The closed form expression of the displacement due to bending and shear is

$$d = P\left[\frac{x^2(L-x)^2}{3EIL} + \frac{(L-x)x}{fLAG}\right] \qquad \text{(Eq. 1)}$$

Using a value of 0.437 for the shear coefficient f, and substituting for A, L, E, I, G and P as below:

A = 1.56 sq. in.	E = 10.0 x 10^6 psi
I = 1.16 in^4	G = 3.75 x 10^6 psi
L = 16.0 in.	P = 1000 lb

the deflection at midspan, x = L/2 is

d = 0.00892 in.

This value is that predicted by the 1D model.

An additional comparison was made from this analysis. The distributions of reactive forces along the supported ends were compared in Table 2A. The 1D model was not included in this comparison, since there is no distribution.

TABLE 2A
DISTRIBUTION OF REACTIVE FORCES

Grid Y-Coord	2D Model	3D Model	C Model	BQ Model
0.	-83.4	-113.3	-82.8	-95.3
2.	-115.7	-91.2	-116.0	-105.2
4.	-101.8	-90.8	-102.3	-99.2
6.	-115.7	-91.2	-116.0	-105.2
8.	-83.4	-113.3	-82.8	-95.3

Eigenvalue Analysis

To compare dynamic response of the five models, the eigenvalues to 3000 Hz were evaluated. Eigenvalues were computed for the stand-alone bench models. The corresponding modal resonances for the different models are listed in Table 3. The simple sdof oscillators are excluded from these models for this evaluation.

TABLE 3
MODAL RESONANCES (Hz)
(Stand-Alone Plate Model)

Mode	1D Model	2D Model	3D Model	C Model	BQ Model
1	851.2	855.1	846.4	846.9	852.6
2	1013.2	1743.7	1649.2	1718.1	1666.4
3	2010.0	2798.0	2376.8	2790.0	2370.7
4	2807.6	2832.2	2727.4	2806.3	2804.8
5	3000.7	3660.8	3542.1	3598.4	3571.4

As a further verification of the accuracy of the models, the MSC/NASTRAN weight generator was used to calculate the masses of the individual stand-alone models. The masses of the models are given in Table 3A.

TABLE 3A
MASS OF MODELS ($lb\text{-}sec^2/in^4 \times 10^{-3}$)

1D Model	2D Model	3D Model	C Model	BQ Model
8.4440	8.2681	8.5210	8.3415	8.5210

Stiffness Analysis

Stiffness of the various models was evaluated by applying a unit displacement at the location of the attachment of the 600-Hz oscillator with the bench. An intermediate node (big foundation mass point) was rigidly attached to the bench support points. The resultant reactions between this intermediate node and the oscillator base were the stiffnesses, and they are listed in Table 4.

TABLE 4
STIFFNESS WITH RESPECT TO 600-Hz OSCILLATOR BASE
(#, in., Rad, sec)

Term	1D Model	2D Model	3D Model	C Model	BQ Model
T3	6.95E4	5.85E4	6.33E4	5.76E4	6.10E4
R1	2.78E5	2.34E5	2.53E5	2.30E5	2.44E5

Random Analysis

For random analysis, the 600-Hz oscillator was included. Eigenvalue extraction was performed to 3000 Hz. The modal resonances extracted for the various models in development of the transfer functions between the base (big foundation mass) and the 600-Hz oscillator are listed in Table 5.

TABLE 5
MODAL RESONANCES FROM RANDOM ANALYSIS (Hz)
(Eigenvalue Extraction to 3000 Hz)

Mode	1D Model	2D Model	3D Model	C Model	BQ Model
1	534.6	588.5	591.5	598.5	594.3
2	918.1	934.6	926.6	934.2	930.5
3	1070.5	1037.1	984.6	1005.7	1039.6
4	1076.2	1048.8	1043.1	1041.3	1058.9
5	2092.7	2495.2	2293.7	2851.7	2236.4

The system was subjected to a random vibration. The vibration specification used was flat (white noise) at 1.0 g^2/Hz from 20 to 2000 Hz with an RMS of 43.359 gRMS. Subjecting a system to this random input results in a random response whose RMS is the magnitude of area under the respective curves of the transfer function (the units, however, not being the same) over the analysis range. Table 6 provides the RMS of the responses developed for the various models at the base of the 600-Hz oscillator and the 600-Hz oscillator mass. Plots of the responses at the 600-Hz oscillator base are shown as Figs. 6 through 10.

TABLE 6
RMS RESPONSE TO RANDOM WHITE NOISE

Location	1D Model	2D Model	3D Model	C Model	BQ Model
Osc Base	155.6	165.4	169.8	175.5	169.1
Osc Mass	240.5	235.5	243.7	240.5	241.5

Random Response to LITE Qualification Input

The case study and comparison performed was used to justify models used in the analysis of the LITE OM. Therefore, it was appropriate that the models be subjected to the LITE qualification random vibration input (Fig. 11).[3] For this analysis, the 840-Hz oscillator was removed from the model. Again, transfer functions were developed based on a Q of 20.0. Table 7 provides the RMS of the responses at the 600-Hz oscillator mass and base. Eigenvalue extraction during analysis is the same as in the previous analysis.

TABLE 7
RMS RESPONSE TO LITE QUALIFICATION-LEVEL RANDOM VIBRATION

Location	1D Model	2D Model	3D Model	C Model	BQ Model
Osc Base	16.2	14.2	14.8	14.9	14.6
Osc Mass	43.4	36.4	37.2	35.9	36.7

Transmissibility Across the Plate

To evaluate transmissibility across the plate, the 840-Hz oscillator was added. A (white noise) 1 g^2/Hz random input from 20 Hz to 2000 Hz with an RMS of 43.359 gRMS was applied at the mass of the 600-Hz oscillator. This load is equivalent to the reaction force developed by a support bracket to a mass oscillating with the given psd acceleration. Subjecting a system to this random input results in a random response with the square of the magnitude of area under the respective curves of the transfer function (the units, however, not being the same) over the analysis range. As a result, the RMS of the random response is the area under the transfer function curve. Table 8 provides the RMS of the responses developed for the various models at the interface with the 600-Hz oscillator and the 840-Hz oscillator. Response at the mass of the 840-Hz oscillator was also developed. The response at the mass of the 840-Hz model is plotted in Figs. 12 through 16.

TABLE 8
RMS RESPONSE TO RANDOM INPUT

Location	1D Model	2D Model	3D Model	C Model	BQ Model
600 Hz Osc Mass	122.2	121.4	121.7	120.9	122.6
600 Hz Osc Base	29.6	33.3	30.0	33.9	31.0
840 Hz Osc Mass	54.2	52.3	52.8	53.0	52.1
840 Hz Osc Base	20.0	22.2	20.9	22.7	21.7

Eigenvalue extraction was performed to 3000 Hz. The modal resonances extracted for the various models in development of the transfer functions between the oscillators supported on the plate are listed in Table 9.

TABLE 9
MODAL RESONANCES (Hz)
(Eigenvalue Extraction to 3000 Hz)

Mode	1D Model	2D Model	3D Model	C Model	BQ Model
1	532.8	524.9	534.7	523.6	535.4
2	738.1	728.8	738.1	725.6	739.3
3	989.6	986.8	970.7	986.6	995.1
4	1018.7	1006.0	1009.2	1006.1	1015.3
5	1023.3	1026.1	1012.4	1020.0	1017.6
6	1400.9	1396.6	1370.4	1396.6	1404.9
7	1447.7	1423.6	1430.2	1423.7	1439.5
8	2100.8	1879.9	1819.8	1855.6	1792.9
9	2225.5	2844.3	2491.5	2802.2	2484.1
10	2819.7	2890.5	2755.9	2897.3	2821.1
11	3974.4	3676.9	3578.5	3614.5	3595.4

V. EFFECT OF REVISED BOUNDARY CONDITIONS

The same five models were analyzed again to determine the effect of a different set of boundary conditions. In this case the entire set of analyses was not repeated; only stiffness and eigenvalues were evaluated. The stand-alone models were constrained against translation along the neutral axis at the three points shown on Fig. 17. Stiffness with respect to the 600-Hz oscillator location and the stand-alone resonant frequencies was determined. These are listed in Tables 10 and 11, respectively.

TABLE 10
STIFFNESS WITH RESPECT TO 600 Hz OSCILLATOR BASE
(Revised Boundary Conditions)

Term	1D Model	2D Model	3D Model	C Model	BQ Model
T3	7.44E4	5.73E4	6.08E4	5.61E4	5.85E4
R1	2.98E5	2.29E5	2.43E5	2.24E5	2.34E6

TABLE 11
MODAL RESONANCES (Hz)
(Revised Boundary Conditions)

Mode	1D Model	2D Model	3D Model	C Model	BQ Model
1	902.9	803.1	767.5	793.2	777.8
2	1161.9	1031.2	985.7	1017.7	997.3
3	2742.2	2339.2	2176.6	2332.9	2164.9
4	2912.3	2372.6	2376.0	2345.1	2369.8
5	3424.7	2817.7	2683.3	2772.9	2716.9

VI. DISCUSSION OF RESULTS

Analyses of the various models with the one-way simple supported span showed reasonably good agreement for the various loading conditions. The sdof oscillator resonances were selected to be within the affected range of each other and the supporting plate. The models with a single layer of CQUAD elements did a better job of predicting resonances and response than did the 1D model. Of these models the BQ model was nearly identical to the 3D model. The reasons for the discrepancies in these models lie with the representation of edge stiffness. The 2D and C models assume that the honeycomb stiffening effect is evenly distributed across the section. In fact, the discontinuity of the ribs has a different stiffening effect on the cover plates as is evidenced by the end reaction distributions shown in Table 2A. The model using CQUAD and CBEAM elements (BQ) places the ribs where they are and tends to provide an approximation of the end reactions which is more consistent with the 3D model. The stiffness of the model using composite material properties (PCOMP) is lower than the other two plate models and the 3D model (see results in Tables 2 and 4). The reason for this is obvious. The difference lies in the representation of the core. The composite section models the core between the inside faces of the face sheets. The other models (2D and BQ) model the core from the centerline of the face sheets. This was specifically done to try to duplicate the results of the 3D model. In other circumstances, these two models could be improved to represent the core more accurately. The 3D model would always overestimate the core stiffness.

In spite of these discrepancies, the transmissibilities of the various models was quite consistent. In fact, for these analyses the bench was represented quite well by the 1D beam model. One noticeable inconsistency was the relaxation of the interface constraint between the oscillator and the bench on the 1D model. This was apparent because of the downward shift in the resonance.

The revised boundary conditions were designed to relax the end restraints of the overall bench model. This effect was evident by the lower stiffness terms from analysis of the 2D, 3D, C, and BQ models. The 1D model showed an increased stiffness. This effect was also evident in the resonant frequencies. This increased

stiffness was due to the decrease in the "effective length" of the 1D model under bending deformation.

These boundary conditions also forced the models to behave more as two-way flat plates. The 1D model is incapable of exhibiting this behavior. For this type of analysis, a two-dimensional model is more appropriate. In fact, in this case, the terms from Tables 10 and 11 for the BQ and 3D models are very consistent.

VII. CONCLUSIONS

For static and dynamic analysis of the honeycomb bench as a simple one-way span, this type of a beam or bar model is probably adequate for all static and dynamic responses. The 1D model may not be adequate to represent the plate under all supporting conditions, particularly in the case where there is two-way flat-plate action.

For the cases where the system exhibits two-way action, a flat-plate analysis is required. Modeling of the system as done in the BQ model using a single layer of CQUAD elements to represent the cover plates and CBEAM elements to represent the ribs will provide a very good representation of the 3D model with the least amount of execution time. In addition, there is no need to develop additional ratios and factors to account for equivalent stiffness or mass. This model would also allow the representation of different thickness closure sheets as well as different thickness cover sheets. As noted earlier, care must be taken when modeling the ribs to account only for material between cover plates. In addition, the shear coefficient must be properly evaluated.

For the types of dynamic loadings and static loadings evaluated here, there is no need to develop more than a 2D model for representation of the honeycomb plate. In fact, the agreement between the BQ model and the 3D model was very good for all of the conditions investigated. The resonant frequencies for the Barbench and the All-Up model should be closer than those presented in Table 1 if the two models are accurate.

For the LITE analysis, the results as developed with the Bar-Bench Model are expected to be within 10% of those developed from the All-Up Model.

REFERENCES

1. Schaeffer, H. G. , MSC NASTRAN Primer Static and Normal Modes Analysis, Schaeffer Analysis Inc., Mt. Vernon, N. H.. 4th printing, 1984.

2. Cowper, G. R., "The Shear Coefficient in Timoshenko's Beam Theory", Journal of Applied Mechanics, pp. 335-340, June 1966.

3. MIT/Lincoln Laboratory "Environmental Test Specification No. ETS-22 (LITE) Engineering Model", LM-161, 24 April 1989.

4. MSC/NASTRAN User's Manual, MSC NASTRAN Version 65C.

APPENDIX
COMPARISON OF RESULTS WITH PCOM PROPERTY USING MAT1, MAT2 AND MAT8

All analyses of the plate using the PCOMP card were based on the material as input on MAT1 cards. A comparison is performed with the displacement analysis using the MAT2 and MAT8 cards.

The differences in the models lies solely in the input to the MAT card for the core. The inputs are provided below.

MAT1
Field

3	4	5	6	7	8	9
E	G		Rho			
4.00E6	1.54E5		1.01E-5			

MAT2
Field

3	4	5	6	7	8	9
G_{11}	G_{12}	G_{13}	G_{22}	G_{23}	G_{33}	Rho
4.40E5	1.32E5		4.40E5		1.53E5	1.01E-5

MAT8

3	4	5	6	7	8	9
E_1	E_2	Nu_{12}	G_{12}	G_{1Z}	G_{2Z}	Rho
4.40E5	4.40E5	0.3	0.0	1.53E5	1.53E5	1.01E-5

Displacements

Analyses have been performed on the model of Fig. 3 under 1000 lb. line loading applied at midspan. The model has been provided with the simple supported

boundary conditions described earlier. The deflection at midspan is given below.

MATERIAL TYPE	DEFLECTION (inch)
MAT1	0.008788
MAT2	0.006854
MAT8	0.008679

The difference between the results with MAT2 and the other material properties lies with the exclusion of shear flexibility in the analysis with MAT2. By evaluation of Eq. 1 shear flexibility can be shown to be significant. Therefore, in this case, use of the MAT2 properties is inappropriate.

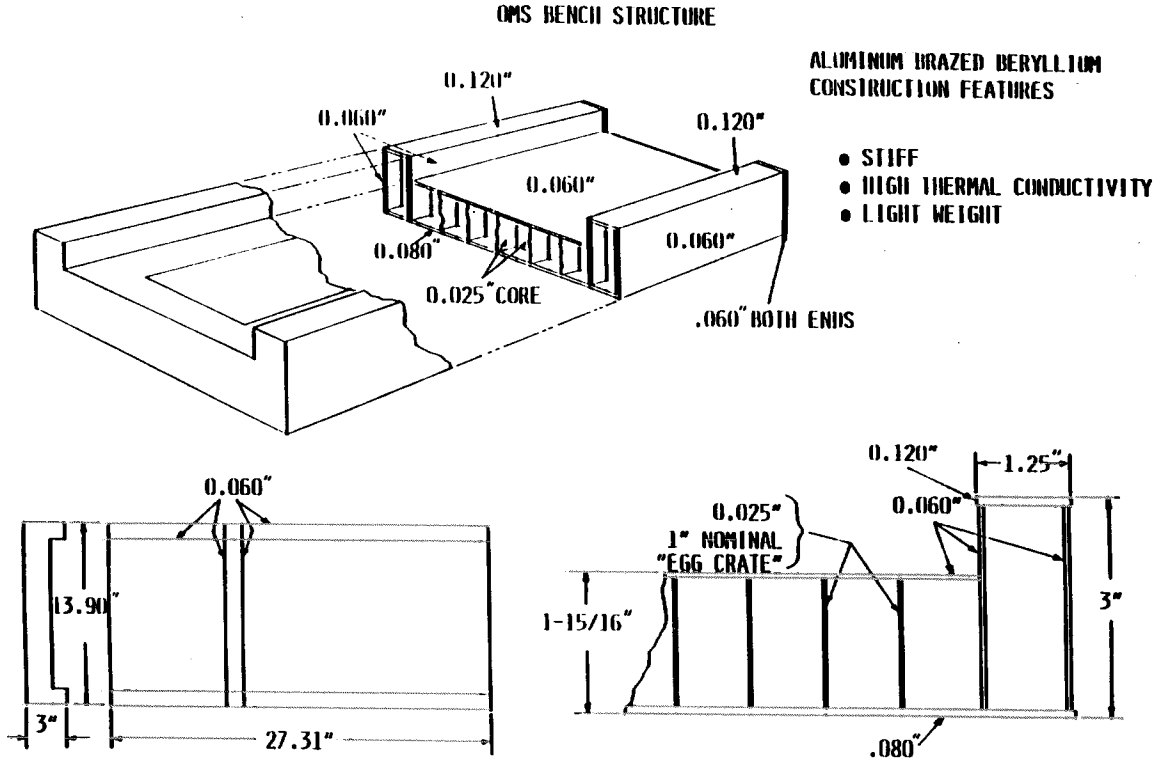

LITE OPTICAL BENCH
FIGURE 1

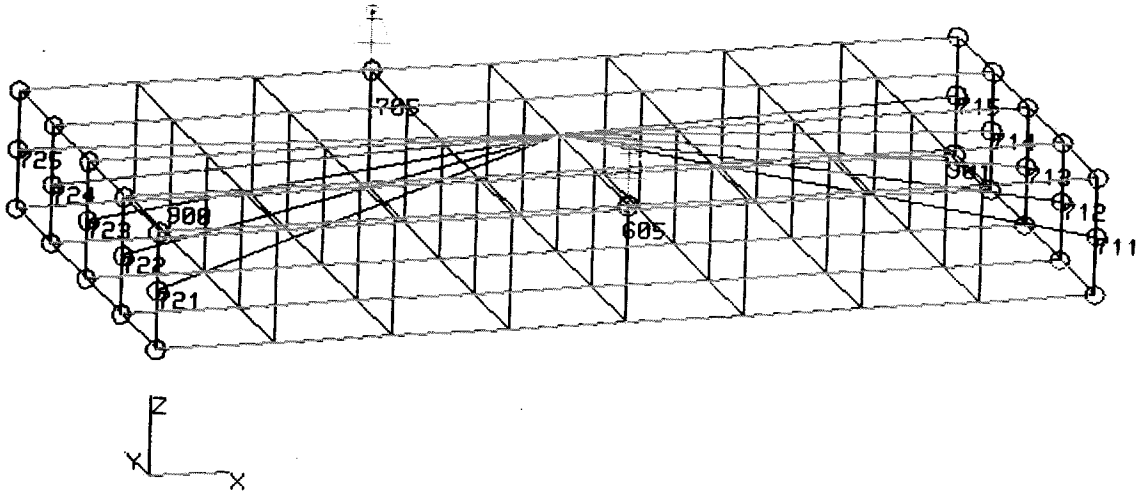

3D MODEL
FIGURE 2

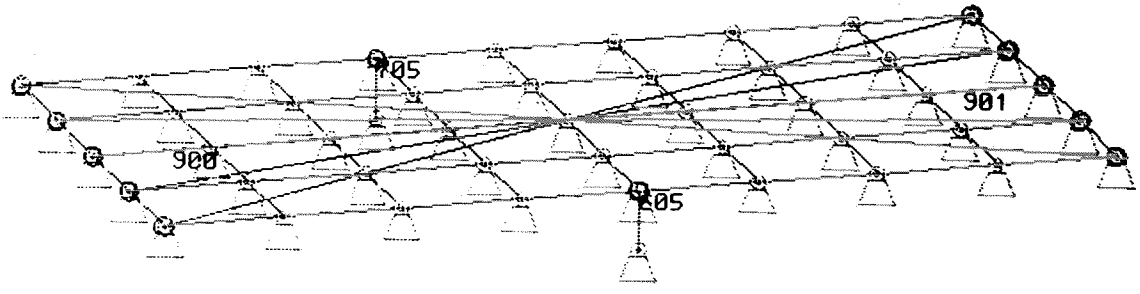

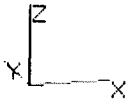

2D MODEL AND C MODEL
FIGURE 3

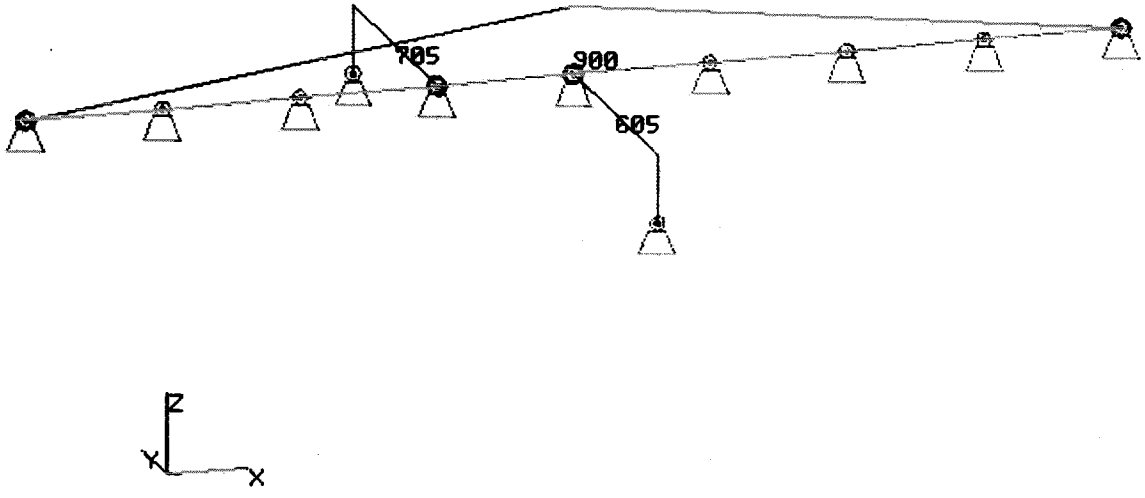

1D MODEL
FIGURE 4

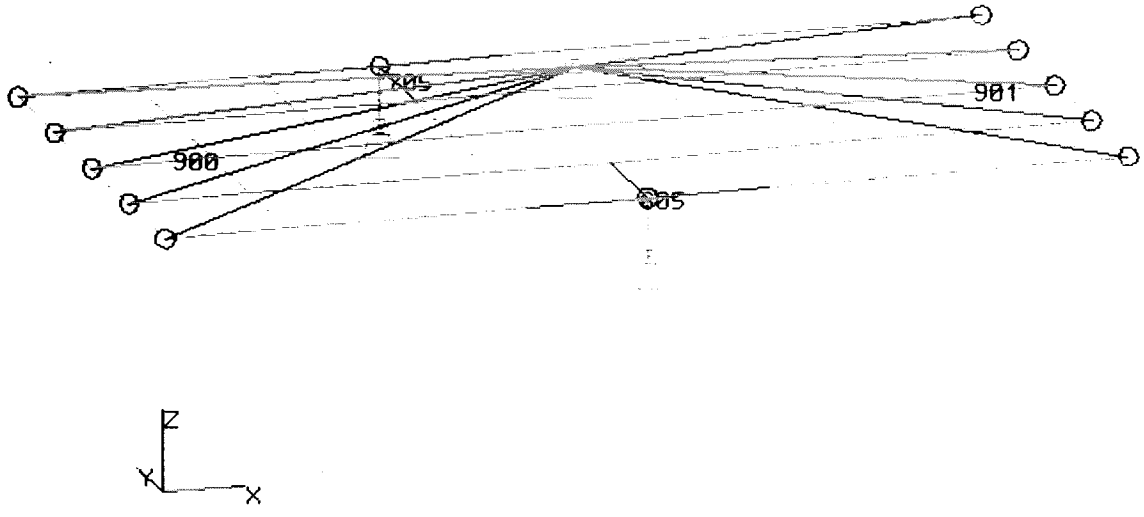

BQ MODEL
FIGURE 5

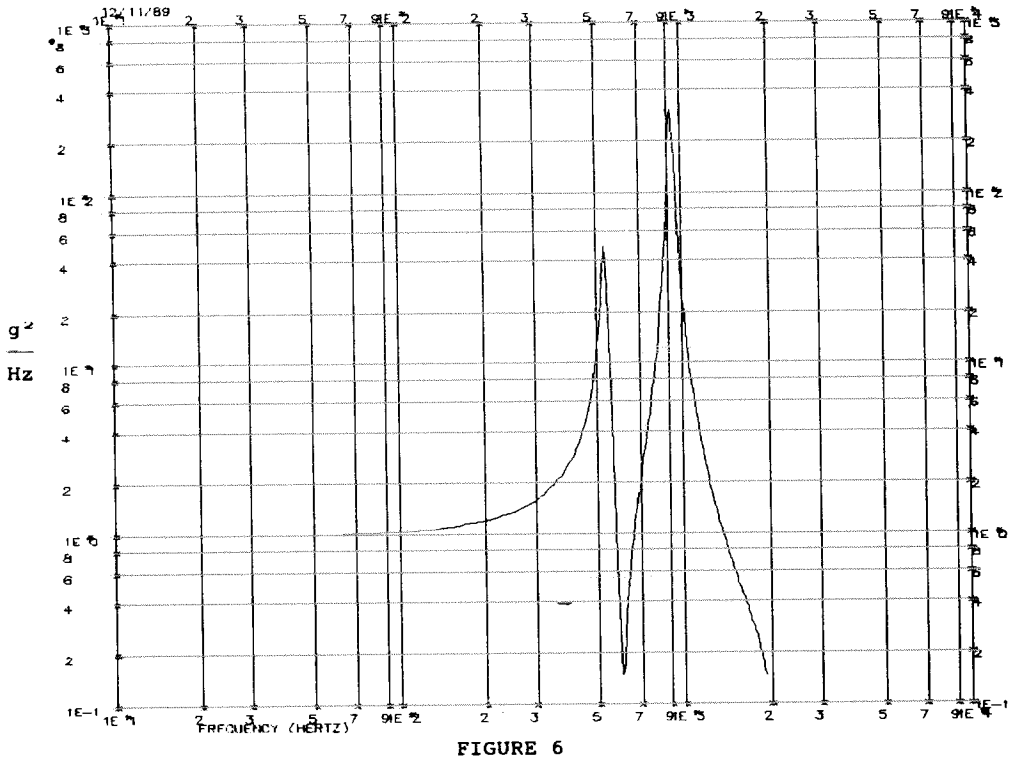

FIGURE 6
1D MODEL
PSD OF ACCELERATION RESPONSE TO WHITE NOISE

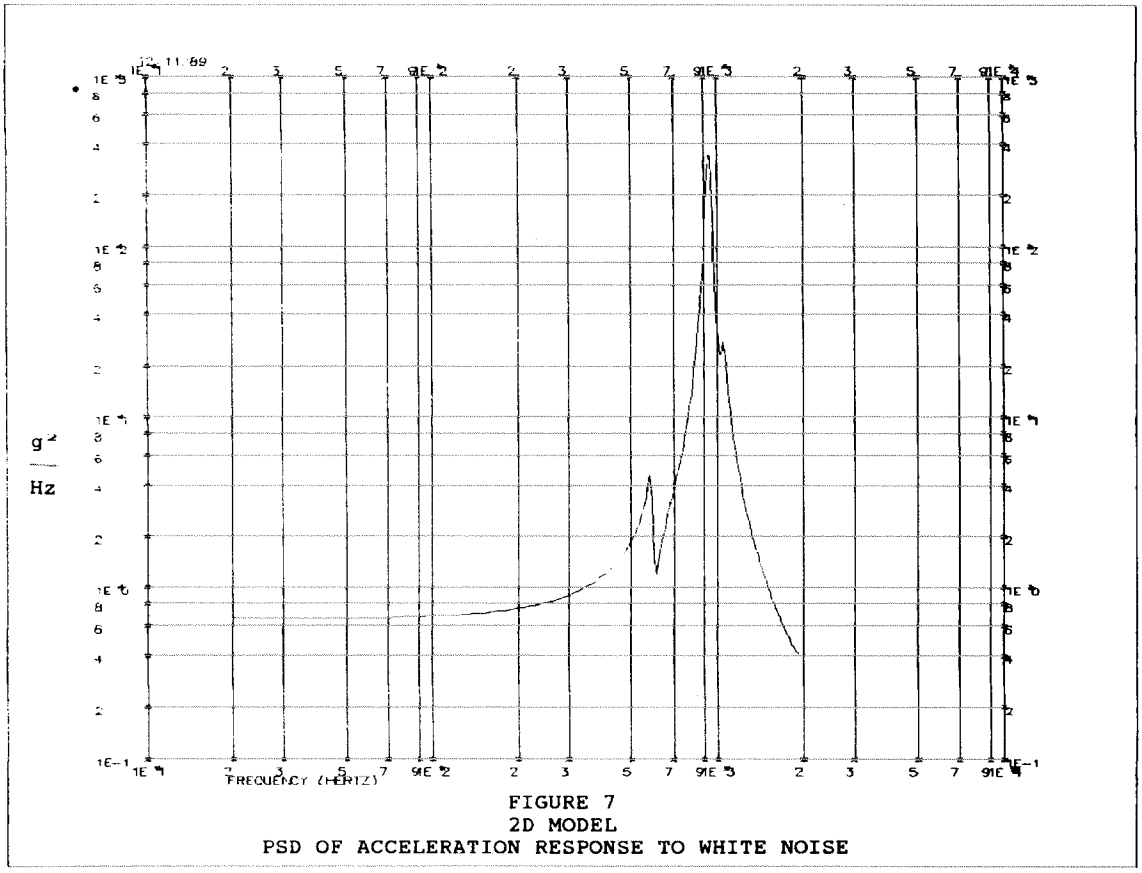

FIGURE 7
2D MODEL
PSD OF ACCELERATION RESPONSE TO WHITE NOISE

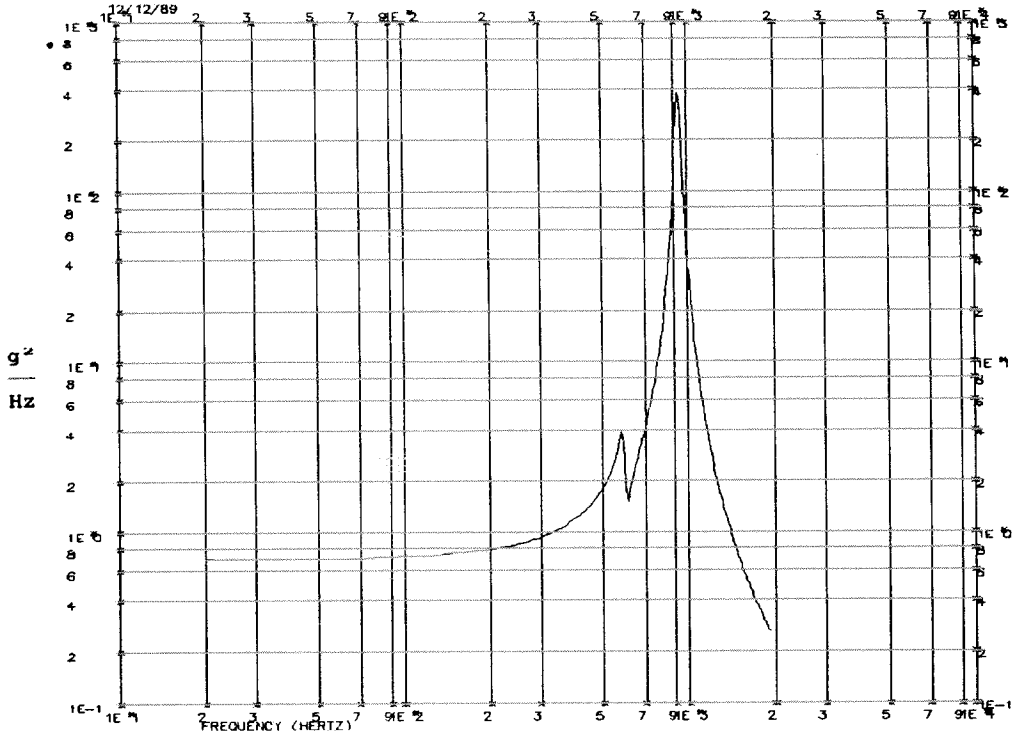

FIGURE 8
3D MODEL
PSD OF ACCELERATION RESPONSE TO WHITE NOISE

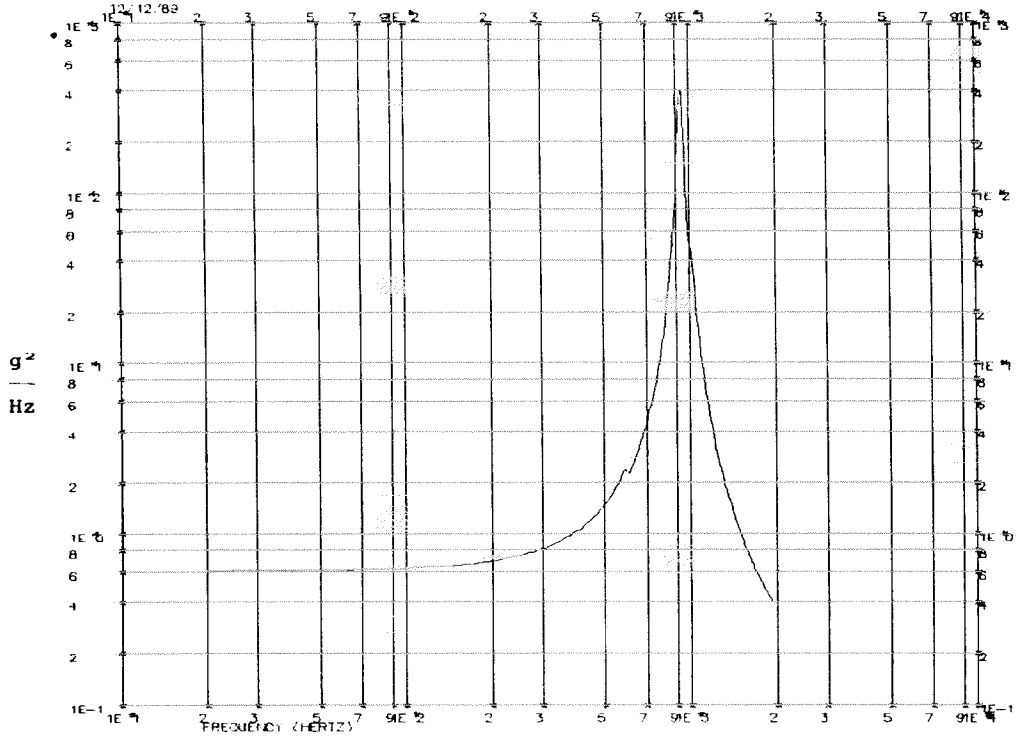

FIGURE 9
C MODEL
PSD OF ACCELERATION RESPONSE TO WHITE NOISE

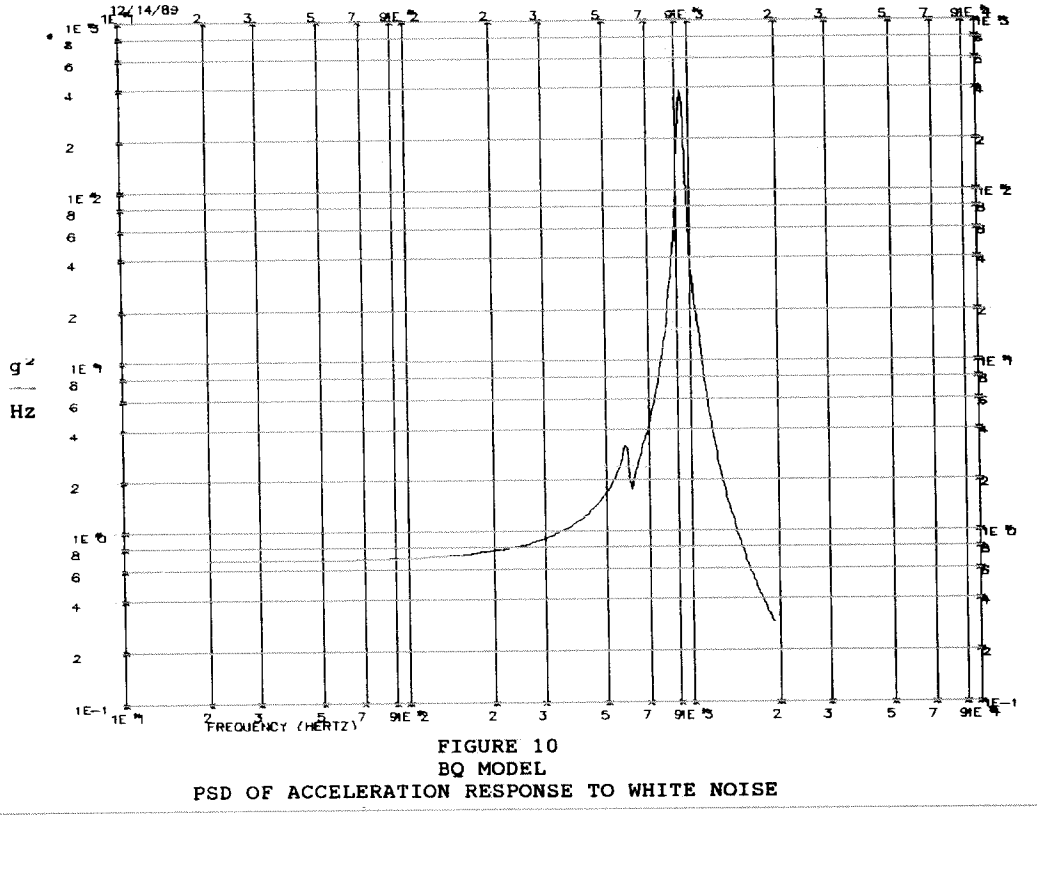

FIGURE 10
BQ MODEL
PSD OF ACCELERATION RESPONSE TO WHITE NOISE

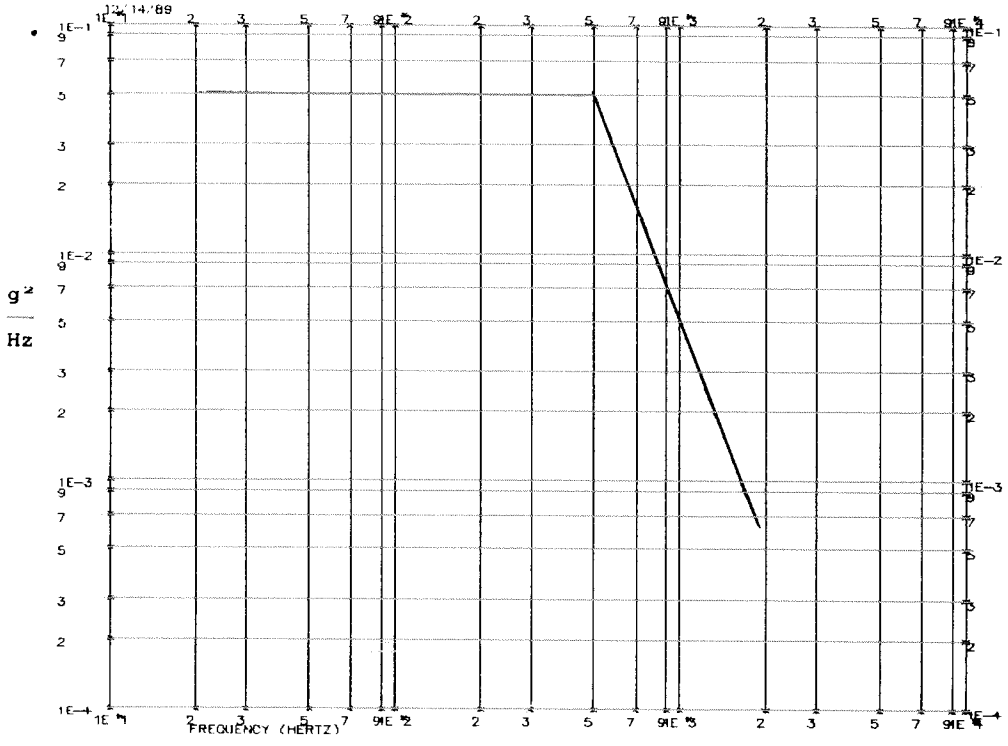

FIGURE 11
PSD OF LITE INPUT

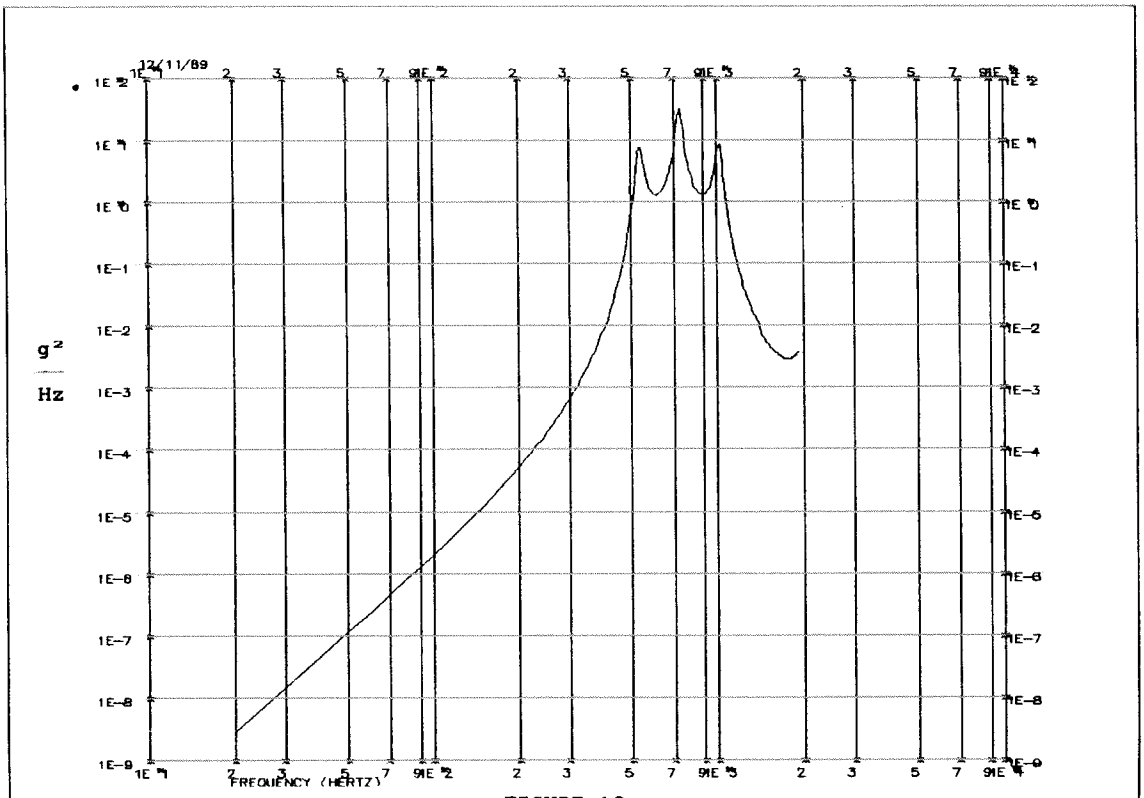

FIGURE 12
1D MODEL
PSD OF ACCELERATION RESPONSE TO WHITE NOISE

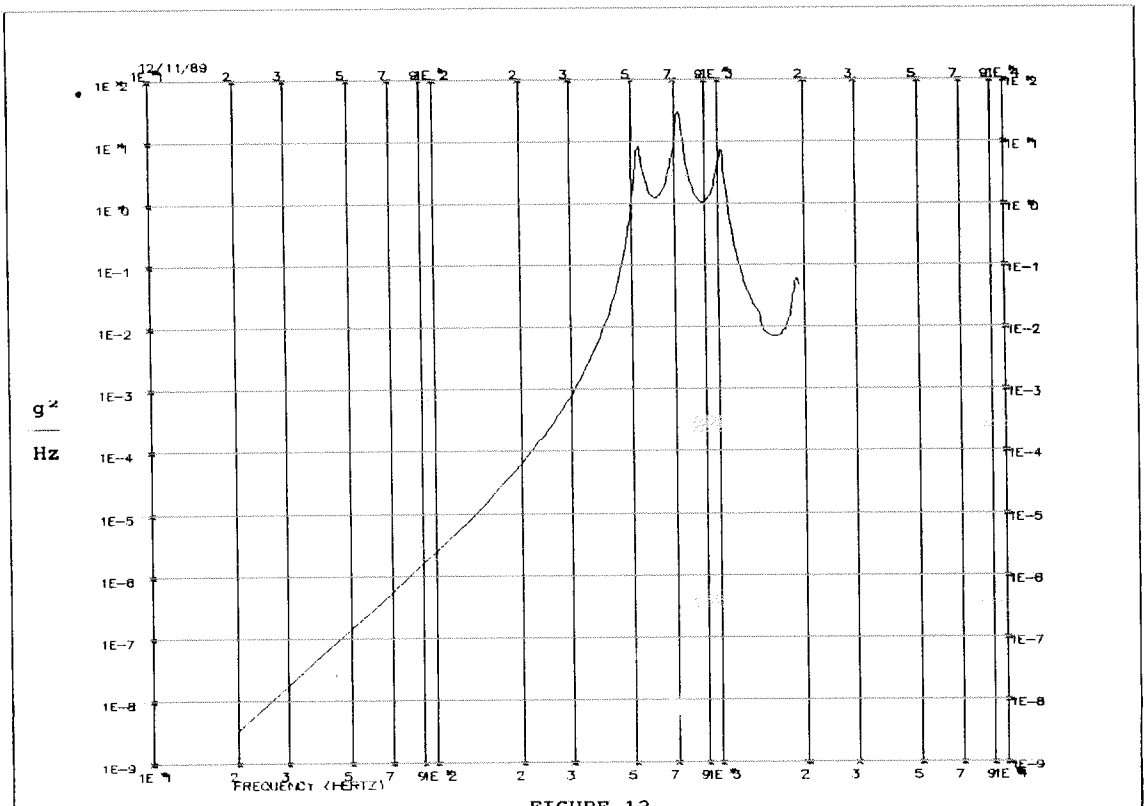

FIGURE 13
2D MODEL
PSD OF ACCELERATION RESPONSE TO WHITE NOISE

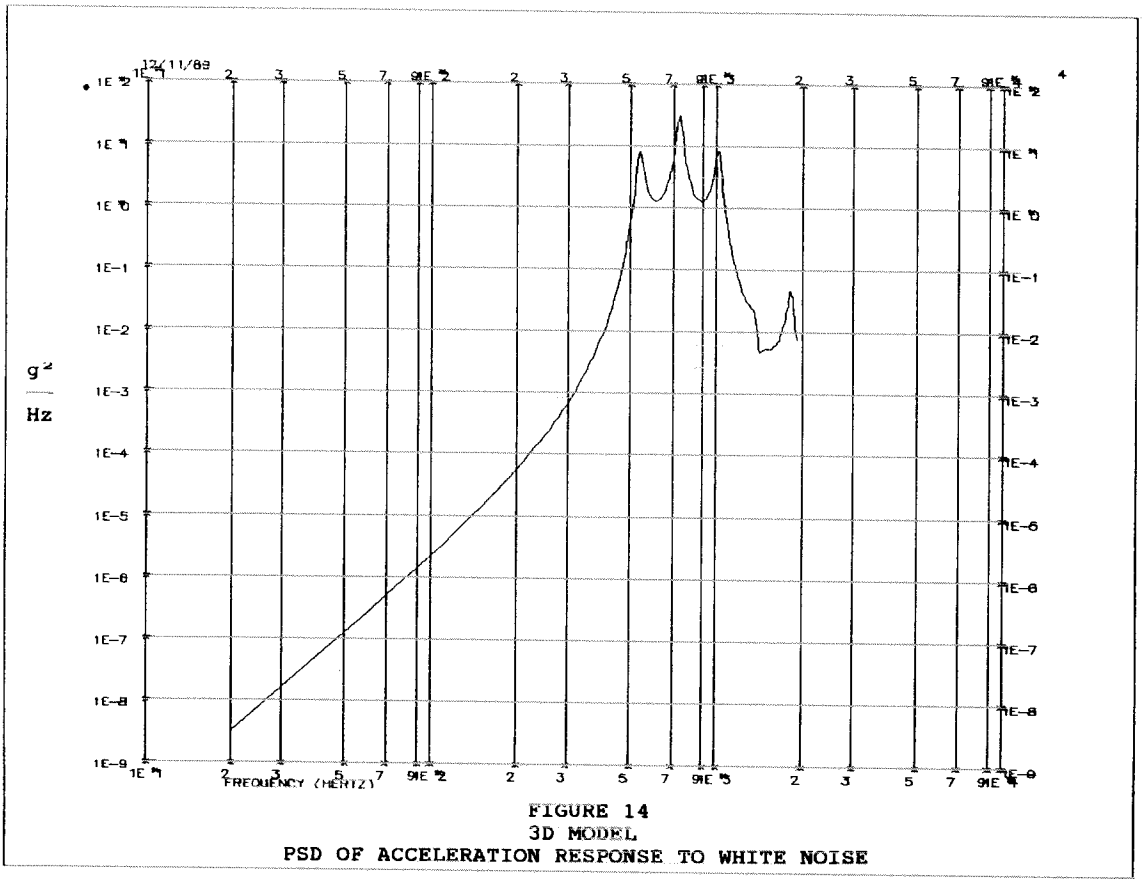

FIGURE 14
3D MODEL
PSD OF ACCELERATION RESPONSE TO WHITE NOISE

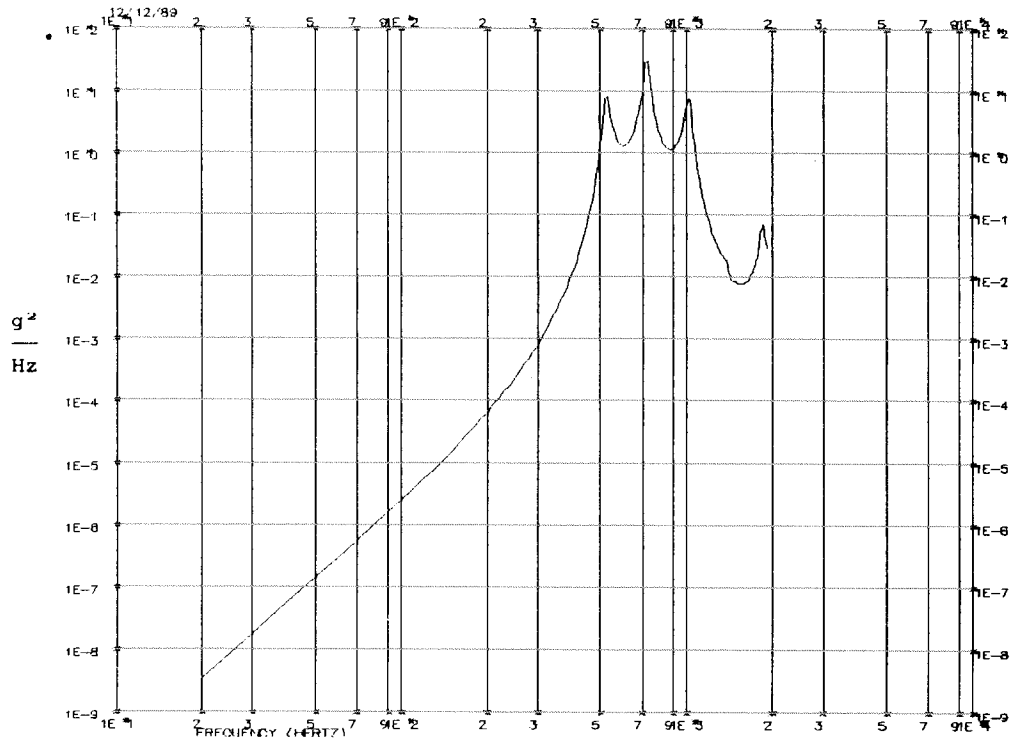

FIGURE 15
C MODEL
PSD OF ACCELERATION RESPONSE TO WHITE NOISE

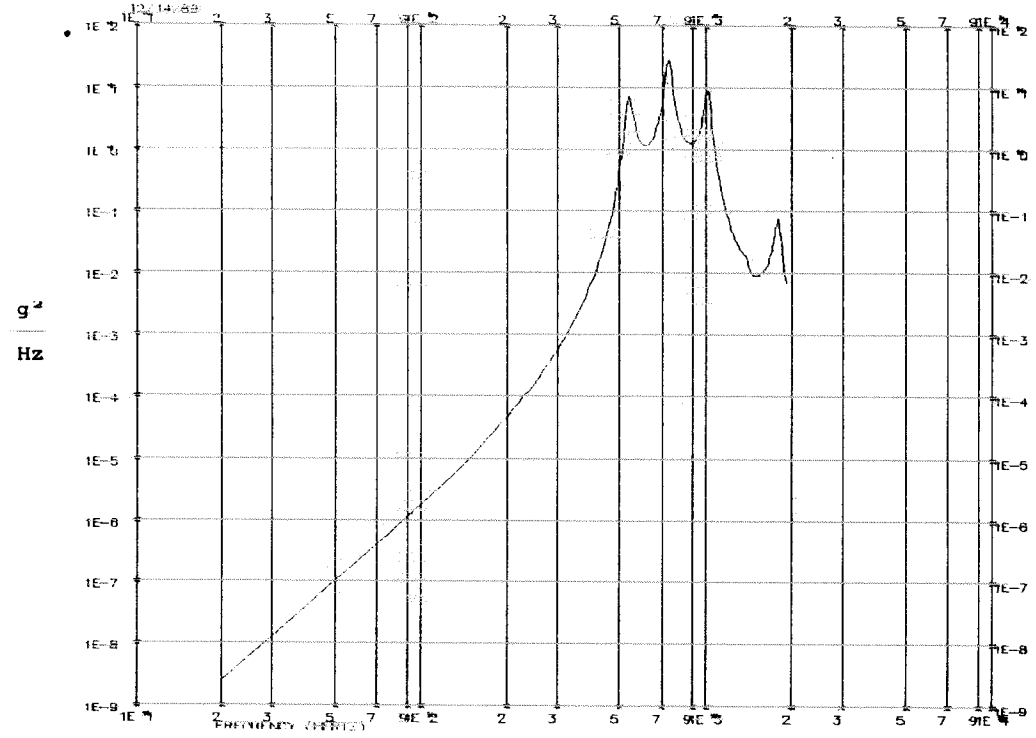

FIGURE 16
BQ MODEL
PSD OF ACCELERATION RESPONSE TO WHITE NOISE

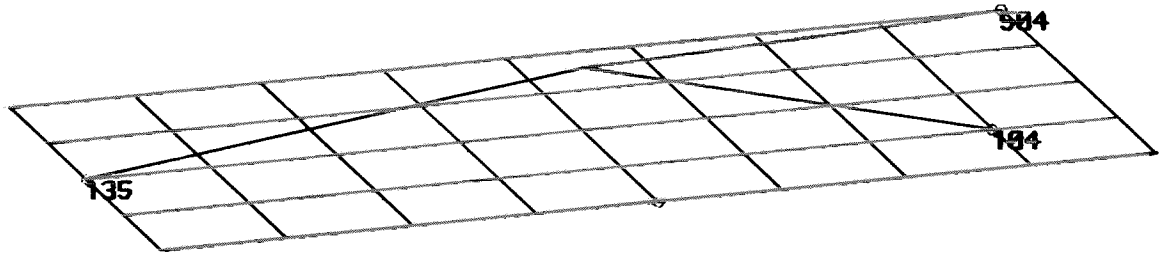

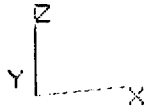

REVISED CONSTRAINTS
FIGURE 17